Natural and Applied Sciences International Journal (NASIJ)

eISSN: 2788-4619 (online)

https://doi.org/10.47264/idea.nasij/3.2.5 Vol. 3, No. 2, (July-December 2022), 53-71

https://www.ideapublishers.org/index.php/nasij



Research Article

Evaluation of the weighted least square based Receiver Autonomous Integrity Monitoring (RAIM) for single frequency GNSS receivers

Sunnyaha Saeed^{1, 2} | Salma Zainab Farooq*³ | Imtiaz Nabi^{1, 2} | Saqib Mehdi⁴

- 1. Department of Space Sciences (GNSS), Institute of Space Technology, Islamabad, Pakistan.
- 2. National Centre of GIS and Space Applications, Institute of Space Technology, Islamabad, Pakistan.
- 3. Department of Electrical Engineering, Institute of Space Technology, Islamabad, Pakistan.
- 4. Institute of Geodesy and Geoinformatics, Wroclaw University of Environmental and Life Sciences, Wroclaw, Poland.
- * Corresponding Author Email: zaineb.farooq@ist.edu.pk

Received: 11-Sep-2022 | Revised: 20-Dec-2022 | Accepted: 23-Dec-2022 | Published: 31-Dec-2022

Abstract

Single frequency receivers for Global Navigation Satellite System (GNSS) are low-cost and easily accessible, deeming them cost-effective for commercial applications requiring localization and tracking. However, the positioning solution these receivers provide must conform to desired reliability standards. A reliability check is essential in the signal-degraded environment, where a position fix might be unacceptably inaccurate. Under such conditions, faulty measurements need to be identified and excluded to ensure the system's integrity and get a reliable solution. In this paper, a Receiver Autonomous Integrity Monitoring (RAIM) scheme is devised that employs different tests. The first test performs a global sweep on all epochs and raises the alarm after detecting the fault. Next, a group of tests are performed to identify the satellite responsible for producing the faulty measurements. Once identified, it is then excluded from the measurements to maintain the reliability of the positioning provided by the receiver. The results indicate that a polling scheme based on multiple tests identifies the faulty satellite correctly and minimizes the false alarm rate if either of these tests is performed individually.

Keywords: GNSS, GPS, RAIM, integrity monitoring, weighted least square, fault detection, fault identification, faulty measurements.

How to Cite: Saeed, S., Farooq, S. Z., Nabi, I., & Mehdi, S. (2022). Evaluation of the weighted least square based Receiver Autonomous Integrity Monitoring (RAIM) for single frequency GNSS receivers. *Natural and Applied Sciences International Journal (NASIJ)*, 3(2), 53-71. https://doi.org/10.47264/idea.nasij/3.2.5

Publisher's Note: IDEA PUBLISHERS (IDEA Journals Group) stands neutral regarding jurisdictional claims in the published maps and institutional affiliations.

Copyright: © 2022 The Author(s), published by IDEA PUBLISHERS (IDEA Journals Group).

Licensing: This is an Open Access article published under the Creative Commons Attribution-NonCommercial 4.0 International License (http://creativecommons.org/licenses/by-nc/4.0/)



1. Introduction

GNSS based positioning is immensely popular in many sectors due to its passive positioning and timing. However, the received GNSS signal has very low power which makes it vulnerable to errors from both natural and man-made sources. Apart from the contribution of satellite clock, ionosphere and troposphere, the signal suffers from various other error sources on the ground such as the multipath effect and receiver noise etc. All these errors dilute the positioning performance of the GNSS and make it less reliable (Angrisano *et al.*, 2012; Kaplan & Hegarty, 2017; Zhu *et al.*, 2018). Dual frequency and multi-constellation receivers are already equipped with different types of correction models that aid the navigation output. However, such types of receivers are usually expensive and therefore, are not the best choice for the low-cost end user applications such as fleet management, drone-based delivery services, etc. Single frequency receivers currently hold 60% of GNSS mass market (Farooq *et al.*, 2020) but their navigation solution is not accurate as the multi-frequency receivers. Integrity monitoring is one of the methods that can be used to make the single frequency receivers reliable for different applications, while still keeping them cost effective.

GNSS performance is monitored with the help of four metrics namely system availability, continuity, integrity and accuracy. Among these parameters, integrity of the system is the most important to monitor because it ensures whether the solution provided by the system can be trusted or not. It can be used for safety critical applications such as aircrafts, ground based autonomous vehicles, fleet management, object tracking etc. Integrity of GNSS can be monitored through installation of separate system such as Satellite Based Augmentation System (SBAS), Ground Based Augmentation System (GBAS), or indigenously at the receiver end through Receiver Autonomous Integrity Monitoring (RAIM) (Santa *et al.*, 2006; Teunissen & Montenbruck, 2017; Sun & Zhang, 2009; Zhu *et al.*, 2020).

Traditionally, GNSS based measurements have been enhanced with the help of RAIM for the aviation sector to meet the International Civil Aviation Organization (ICAO) standards. Different studies on the identification of faulty measurements are available in the literature since 1980 (Hawkins, 1980). In 1986 Lee devised a range comparison and position comparison method. The author proved that the two methods are mathematically equivalent. However, the results from this study provided evidence that these comparison methods alone are insufficient for identifying faulty satellite. However, combination with additional measurements such as user clock bias estimate monitoring, has some potential to detect the user position error. The author Sturza (1988) further extended RAIM model by using parity method on current measurements. During this study the probability of false alarm and missed detection were related to each other, along with the measurement observation matrix and the ratio of detectible bias shift to standard deviation of measurement noise.

Parkinson and Axelrad (1988) presented a new method for satellite failure detection and isolation. The range residual was used as test statistics for the algorithm presented in this study. Range comparison method was further improved for standalone navigation by Lee (1992) and different baseline RAIM methods were explained in Brown (1992). The authors Hewitson and Wang (2006) assessed the performance levels of GNSS RAIM along with reliability measure and in (Rakipi *et al.*, 2015) implementation of improved fault detection and exclusion algorithm using parity method is explained. Furthermore the advancements in RAIM algorithms and equivalence proof of weighted least square residual and weighted parity method in RAIM are

mentioned in (Blanch *et al.*, 2015; Joerger & Pervan, 2013; Ma *et al.*, 2019). The algorithms used in all these papers are based on conventional RAIM which utilizes a single technique for the fault detection and identification. This research aims to develop a reliable RAIM technique for single frequency GNSS receivers. The RAIM model presented in this research paper detects a faulty measurement in epochs on the basis of two tests: Protection level check and global test. The error causing satellite is then identified on the basis of three tests: Least Square Residual (LSR) test, correlation coefficient and correlation distance.

2. RAIM methodology

The RAIM techniques can be broken down into two main components. The first one is Fault Detection and Exclusion (FDE) while the next one is Position and Protection Levels (PL) calculation. FDE helps to exclude the faulty satellite and then allows the system to maintain the integrity of the positioning. The inputs to RAIM algorithm are standard deviation, measurement geometry, probabilities of false alarms P_{FA} and probability of missed detection P_{MD}. A global test is used for the fault detection while the local test is used for identification of the erroneous measurements. Both tests require a decision threshold which is a critical value for its computation. This decision threshold can be calculated from the probability of false alarm and probability of the missed detection (Kuusniemi, 2005; Rakipi *et al.*, 2015). Furthermore, the RAIM depends on the geometry of the visible GNSS Satellite Vehicles (SV). The minimum requirement for the detection of fault is 5 satellites while exclusion requires a minimum of 6 satellites. However, this minimum requirement is not sufficient since the final subset formed by eliminating one SV at a time must have sufficient geometry for the fault detection capability.

Overall, the navigation system error should be confined within a certain range. This range is called Protection Level (PL) which can be classified as Vertical Protection Level (VPL) and Horizontal Protection Level (HPL). Moreover, HPL and VPL are inversely proportional to positioning accuracy which means greater the accuracy of the system, the smaller will be its protection level. Now, whenever a navigation system is at fault, its navigation accuracy will reduce. Under such condition, the measurements will exceed the protections levels and a warning will be generated (Imtiaz *et al.*, 2019).

3. RAIM Algorithm

3.1. Methodology

The proposed RAIM scheme is based on fault detection and exclusion principle using weighted least square algorithm. During this research, measurements from only one constellation i.e., GPS are used. The algorithm is based on linearized Gauss — Markov model of geodetic adjustment for m number of known measurements and n number of unknowns (Farooq $et\ al.$, 2020). Suppose the receiver has tracked m number of satellites then the equation can be formulated as follow:

$$y = Ax + v \tag{1}$$

y represents $m \times 1$ vector of observed minus computed pseudorange also known as measurement vector, A represents the satellite to user direction cosine vector of $m \times 4$ whose

fourth column consists of 1, which represent the receiver clock bias. While x is 4×1 vector represents the unknowns containing user positioning coordinates x, y, z and clock bias b and v is the $m\times1$ measurements error vector containing both deterministic and random errors. The above equation is solved using least square which is given as:

$$\hat{\mathbf{x}} = (\mathbf{A}' \mathbf{Q}_{\mathbf{y}}^{-1} \mathbf{A})^{-1} \mathbf{A}' \mathbf{Q}_{\mathbf{y}}^{-1} \mathbf{y}$$
 (2)

In equation (2) Q_y size $m \times m$ represents the diagonal weight matrix whose elements are the reciprocal of variance of each measurement error (Blanch *et al.*, 2015). The least square adjustment yields measurement residual which is as under:

$$\hat{\mathbf{v}} = \mathbf{y} - A\hat{\mathbf{x}} \tag{3}$$

$$\hat{\mathbf{v}} = \mathbf{y} - A(A' \mathbf{Q}_{\mathbf{v}}^{-1} A)^{-1} A' \mathbf{Q}_{\mathbf{v}}^{-1} \mathbf{y}$$
 (4)

The variance covariance matrix of the residual can be calculated using Gauss error propagation law which results a $m \times m$ matrix.

$$Q_{v} = Q_{y} - A(A'Q_{y}^{-1}A)^{-1}A'$$
(5)

 Q_v Shows the influence of error vector on measurement residual vector ($\hat{\mathbf{v}}$). Q_v is also known as sensitivity or mapping matrix whose dimension is $m \times m$. Faulty measurement can be detected and identified by residual vector through the mapping Q_v , as both the residual vector and measurement error vector are linearly related.

3.2. Fault detection method

For fault detection, global test is performed. The test statistic is formulated as weighted sum of squares of the least square residual divided by difference between the number of available satellites and number of unknowns also known as redundancy (m-n) (Wang *et al.*, 2018).

$$SSE = \frac{\hat{\mathbf{v}}' \mathbf{Q}_y^{-l} \hat{\mathbf{v}}}{m - n} \tag{3}$$

For integrity monitoring, fault detection is a key factor which is based on the hypothesis testing of global test. The general form of hypothesis tests can be expressed as follow:

$$H_0: SSE \le T \setminus H_1: SSE > T$$

$$(7)$$

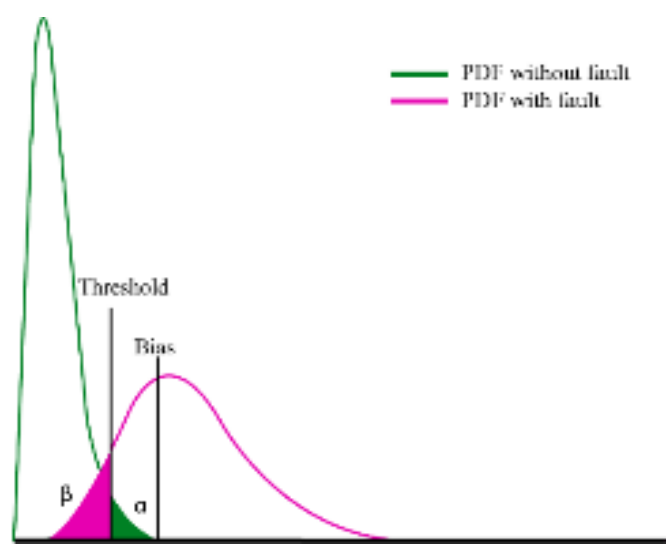
Fault detection is carried out by comparing test statistics and identification threshold. H_0 shows the null hypothesis when no fault is detected and H_1 shows the alternate hypothesis when fault is identified.

For testing measurement inconsistency, both central F-distribution $F_{I-a}(m-n,\infty,0)$ and chi-square test $\chi_{I-a,m-n}$ can be alternatively used in RAIM, where α is the significance level (i.e., false alarm rate). Thereby, for this research, chi-squared test is used to ensure the null hypothesis with respect to alternate hypothesis. If the test statistics are exceeding the threshold value, as in equation (7), an erroneous measurement is detected, and null hypothesis is rejected. After the detection of erroneous measurement, outlier is identified and eradicated. The value of threshold should be determined from chi-square distribution.

$$SSE > \chi_{1-\alpha,m-n} \tag{8}$$

The value of threshold obtained depends upon the probability of false alarm (P_{FA}) and redundancy of satellites. Figure 1 represents the relationship between the probability of false alarm $\alpha = P_{FA}$ and probability of missed detection $\beta = P_{MD}$.

Figure 1: Chi-squared distribution for RAIM



3.3. Fault identification testing

3.3.1. Least Square Residual (LSR) test

Once the error is detected through chi-square test, identification and exclusion of error is necessary for reliable positioning. For fault identification the local test is based on LSR testing. So, if alternate hypothesis of global test is accepted, local test is performed for identification and exclusion of error. The error is assumed to be normally distributed. Test statistic is calculated for *i*-th measurement as:

$$w(i) = \frac{\mathbf{c}' \mathbf{Q}_{y}^{-l} \hat{\mathbf{v}}}{\sqrt{\mathbf{c}' \mathbf{Q}_{y}^{-l} \mathbf{Q}_{y} \mathbf{Q}_{y}^{-l} \mathbf{c}}}$$
(9)

where c is $m \times 1$ vector consisting of zeros with a single 1 as i-th element (Teunissen, 1990). LSR test identifies error when $\left|w(i)\right| > N_{\frac{\alpha_0}{2}}(0,1)$, i-th measurement is considered as unreliable/erroneous and excluded from processing. A single outlier in one observation tends to increase several values of |w(i)| but the measurement with largest value higher than threshold is considered as an outlier (Zhang *et al.*, 2019). α_0 is the significance level of the local test which is predefined as per the required application. The value of both parameters of significance level of global and local test is predefined, both the parameters are interrelated, along with the probability of missed detection β , which remains same for both tests. In order to ensure an accurate fault detection, correlation analysis methods are used in addition to LSR test to detect and eliminate erroneous measurements.

3.3.2. Correlation analysis method

Correlation analysis is concerned with examining the relationship between two variables, or to put it more simply, measuring the degree of correspondence between two random variables. In fault identification, correlation analysis is performed to identify the erroneous measurement by measuring the degree of correspondence between measurement residual vector \hat{v} and measurement error vector \mathbf{v} , and the relationship between these vectors is:

$$\hat{\mathbf{v}} = \mathbf{Q}_{\mathbf{v}} \mathbf{v} \tag{10}$$

The value of q_{y} can be expressed as follow:

$$Q_{v} = \begin{bmatrix} Q_{11} & Q_{12} & L & Q_{1n} \\ Q_{21} & Q_{22} & L & Q_{2n} \\ M & M & O & M \\ Q_{m1} & Q_{m2} & L & Q_{mn} \end{bmatrix}$$
(11)

In order to measure the degree of correlation, two factors are considered: correlation coefficient and distance correlation. The correlation coefficient c(i) of Q_v and \hat{v} is calculated by given formulae:

$$c(i) = \frac{\sum_{j=1}^{m} (Q_{v,i}(j) - \overline{Q}_{v,i})(\hat{v}(j) - \overline{\hat{v}})}{\sqrt{\sum_{j=1}^{m} (Q_{v,i}(j) - \overline{Q}_{v,i})^2 \sum_{j=1}^{m} (\hat{v}(j) - \overline{\hat{v}})^2}}$$
(12)

And distance correlation d(i) is calculated as:

$$d(i) = \sqrt{\frac{1}{m} \sum_{j=1}^{m} Q_{v,i}(j) - \hat{v}(j))^{2}}$$
(13)

Where i=1,2,...,m, $Q_{v,i}$ is the transpose of i-th column of Q_v , and $Q_{v,i}(j)$ and $\hat{v}(j)$ is the j-th element of $Q_{v,i}$ and \hat{v} . $\bar{Q}_{v,i}$ and \bar{v} are the mean of $Q_{v,i}$ and \hat{v} respectively. Correlation

analysis method implies the following two tests for identification of outlier. The highest value of absolute correlation co-efficient and the smallest value of correlation distance is considered as outlier (Zhang *et al.*, 2019).

After the fault detection and identification, the results of all the identification tests are compared. Identification tests: LSR test, correlation-coefficient and distance correlation are named as k1, k2 and k3. A polling scheme is implemented such that if all the three tests identify the same outlier, it is excluded and the user position is recalculated.

3.4. Protection level

A GNSS receiver's reliability must always be determined by the amount of trust, applications are able to place in the system at any given time. To improve the accuracy of the position information and keeping people and assets safe, the GNSS receiver calculates the protection level. A receiver's PL describes the maximum possible position error (in units of distance) within a specified confidence level which is also taken as a threshold for fault detection. The PL represents the radius of the circle having the true position as its center (Hewitson & Wang, 2006; Wang *et al.*, 2018; Zheng *et al.*, 2018). Horizontal protection level (HPL) provides bounds to horizontal direction and Vertical Protection Level (VPL) provides bounds to vertical position. HPL is determined as:

$$HPL = HSlope_{max} \times P_{bias}$$
 (14)

Where $HSlope_{max}$ is the maximum horizontal slope and P_{bias} is the minimal detectable bias. $HSlope_{max}$ represents the degree of sensitivity to bias in the horizontal position error for any pseudo range measurement and is formulated as (Wang *et al.*, 2018; Zabalegui *et al.*, 2020):

$$HSlope_{i} = \sqrt{(M_{1i}^{2} + M_{2i}^{2})/Q_{V}(i)}$$
 (15)

Here $\mathbf{M} = (\mathbf{A'Q_y^A})^{-1} \mathbf{A'Q_y^A}$ and $\mathbf{M_{1i}}, \mathbf{M_{2i}}$ are *i*-th column values for 1st and 2nd rows respectively. The squared sum of $\mathbf{M_{1i}}, \mathbf{M_{2i}}$ is divided by the corresponding diagonal value at *i*-th place in the $\mathbf{Q_v}$ matrix. \mathbf{M} shows that geometry matrix and HPL are highly correlated and $\mathbf{Q_v}$ is the sensitivity matrix calculated as in equation (5). P_{bias} is determined by setting the threshold in the failure detection test, probability of missed detection and variance σ_Q .

$$P_{bias} = \sqrt{\lambda} \times \sigma_{\circ} \tag{16}$$

where λ in equation (16) represents the non-centrality parameter of the chi-square density function as obtained from (Baarda, 1968). Protection levels for each application varies, because of the desired reliability of the GNSS receiver and of position estimate.

The flow chart for the implemented RAIM methodology is shown in Figure 2. It should be noted that for fault detection two tests are performed. The first test, SSE > PL, is to check

whether the test statistics are greater than the PL for position to be calculated which represents an error. The second test is the global test in which test statistics are compared with central chi-square distribution. After that the exact satellite, causing the fault, is identified by the local test, which is composed of three different tests including LSR, correlation coefficient and correlation distance as mentioned earlier.

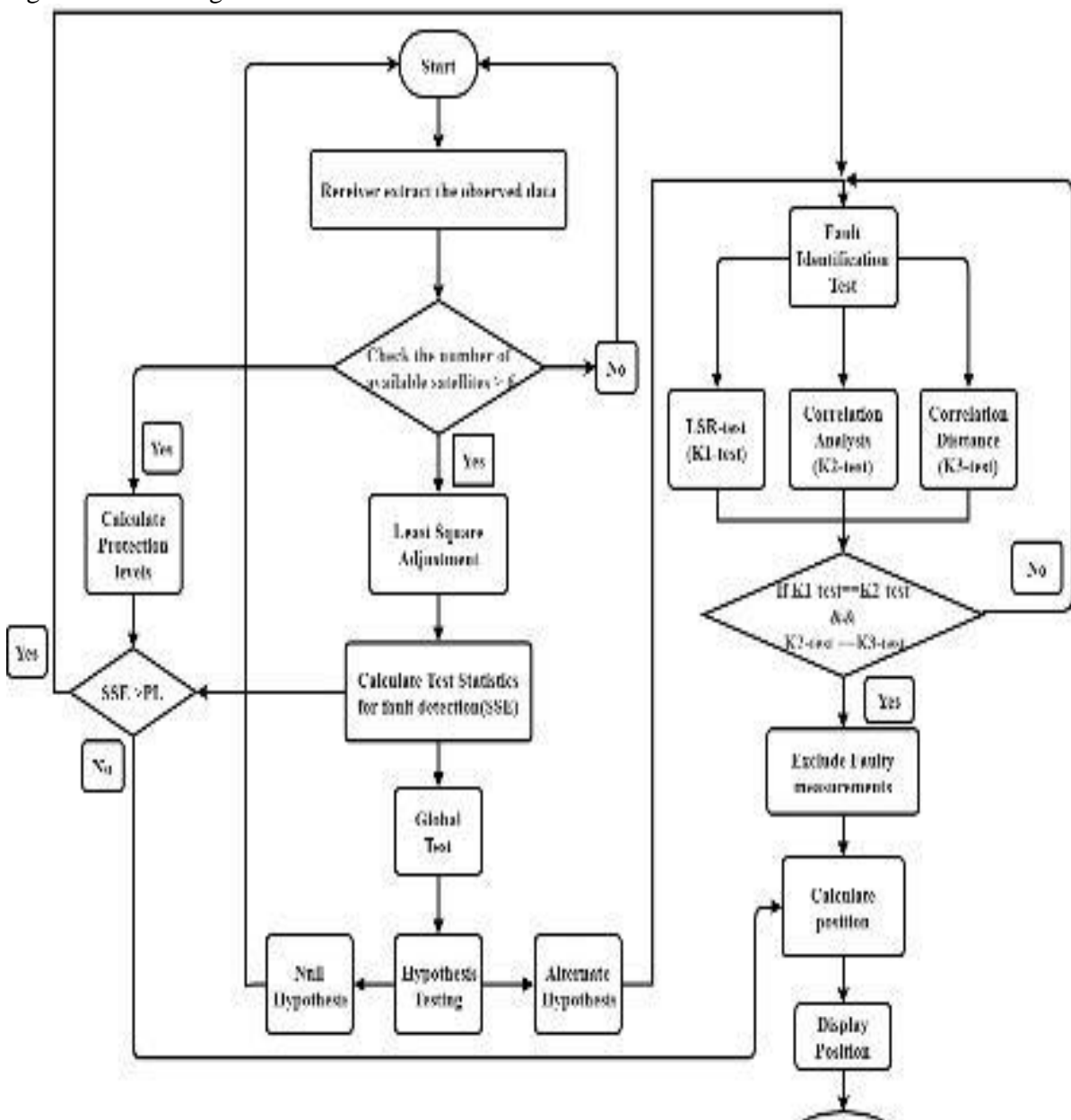


Figure 2: RAIM algorithm

4. Experimental setup, results, and discussion

During this experiment the u-blox C94 M8P receiver was used which is a single frequency receiver that supports GPS, GLONASS, and Quasi Zenith Satellite System (QZSS). For the algorithm verification two data sets were collected under clear sky in the Khatana Stadium at the Institute of Space Technology (IST), Islamabad, Pakistan. The receiver was configured on

cud

single positioning mode with an elevation mask of 10 degrees to maintain a good satellite geometry and reduce the effect of multipath from the surrounding. The sampling frequency was set to 1 Hz and only GPS satellites were selecting during the data collection. The details for both the datasets are given in Table-1, while the location and track of both datasets is shown in Figure 3.

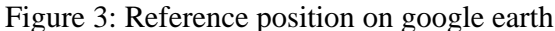




Table-1: Different data sets collected for experiments

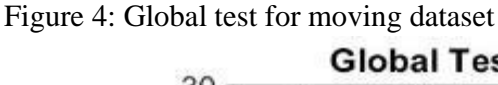
Dataset	Location	Date	No. of Epochs	Visible Satellite (PRN)
Data set-1	IST Khatana	28-Feb-2022	600	13,15,17,28,30,14,19,1,24
Data set-2	Stadium	2 nd -June-22	287	32,22,10,23,21,31,27,8,24,18,1

A total of 9 GPS satellites were visible in data set-1 and 11 satellites in data set-2 at the time of data collection. The data were received in ubx format which is standard binary output of ublox receivers. It was converted to Receiver Independent Exchange (RINEX) for post processing in MATLAB. For detection and identification, thresholds are calculated using the chi-squared distribution and normal distribution using the probability of false alarm and missed detection. For which significance level α and α_0 are predefined to 0.1% and value of β is chosen 80% as in (Baarda, 1968).

4.1. Experiment for datasets

The proposed algorithm is applied for both datasets. During the processing of data set-1 an error was intentionally introduced in epoch 400 and onwards in pseudo range of PRN 17 and checked through FDE procedure. After least square adjustment, global test was applied for fault detection during which the test statistics were found to be exceeding the threshold and as a result, an alarm was generated. In Figure 4 the result of the global test can be seen clearly at epoch 400 and onwards for PRN 17. Alternatively for fault detection, protection level can also be set as a threshold and compared with test statistics SSE and alarm is generated when SSE exceed the protection level as shown in Figure 5.

Once the fault was detected the next step was to identify the erroneous measurements which was done through a combination of local tests based on LSR testing and correlation analysis. During these tests the test statistics for local test were found to be exceeding the threshold in the exact epoch in which the error was introduced intentionally as seen in Figure 6. The results of LSR test, correlation distance, and correlation coefficient can be found in Table-2. The maximum value of LSR test and correlation coefficient, and minimum value of correlation distance represents the error in the pseudo range of PRN 17. The last step of the algorithm is to exclude the faulty measurements from the position calculation. For this purpose, multiple tests need to point to the same satellite. The impact of faulty measurements before and after exclusion, can be observed in the Figure 7. Similarly, the variation in X, Y, and Z coordinates can also be seen in Figure 8 for before and after RAIM.



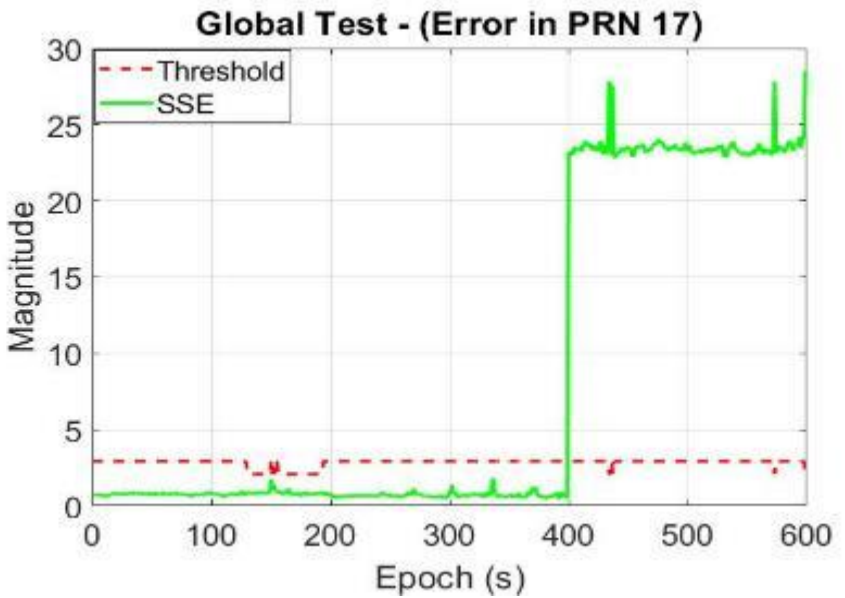


Figure 5: Comparison of Protection Level (PL) with test statistics

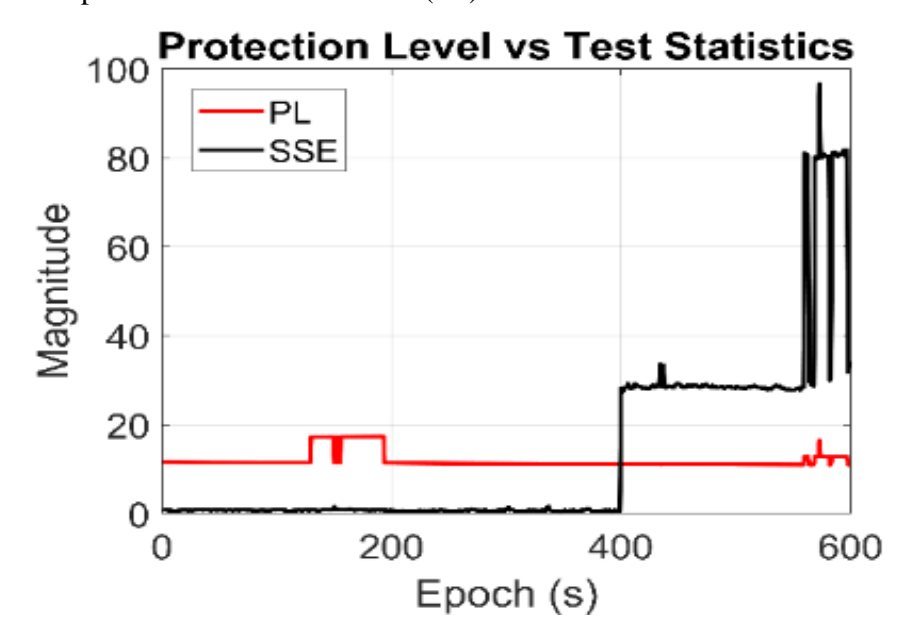


Figure 6: Local tests for the identification of faulty satellite

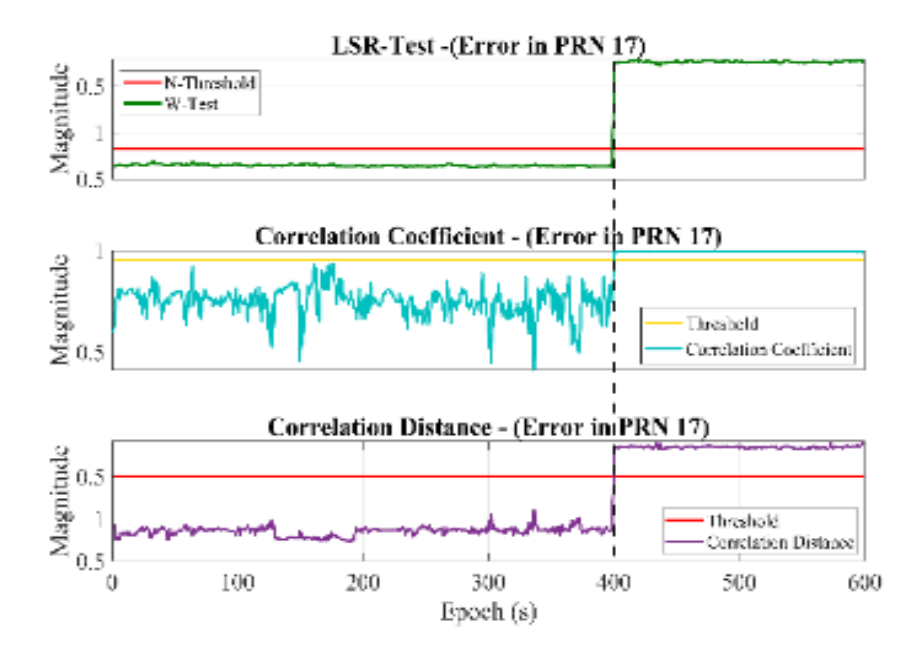
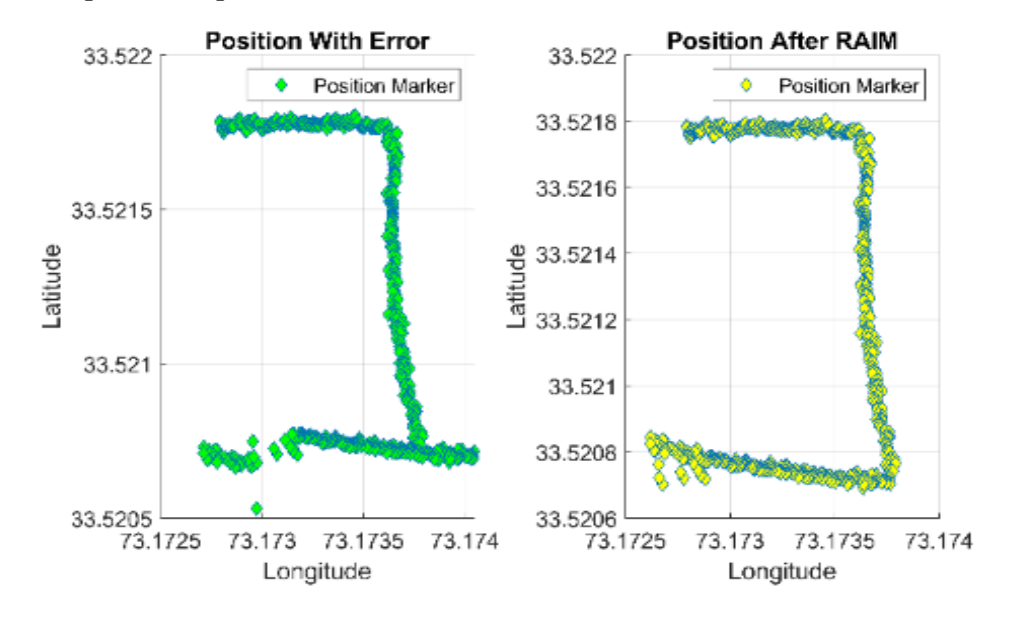


Table-2: Test results for fault identification (moving dataset)

Satellite (PRN)	LSR Test	Correlation Coefficient	Correlation Distance
13	2.9247	0.0690	31.54
15	1.5923	0.1264	32.23
17	19.7897	0.9988	25.76
28	9.3983	0.4346	34.49
30	4.3466	0.2230	33.31
14	9.5721	0.4781	34.60
19	2.3972	0.1350	31.25
1	2.8382	0.1819	33.95
24	0.7135	0.0157	31.87

Figure 7: Comparison of position with and without error



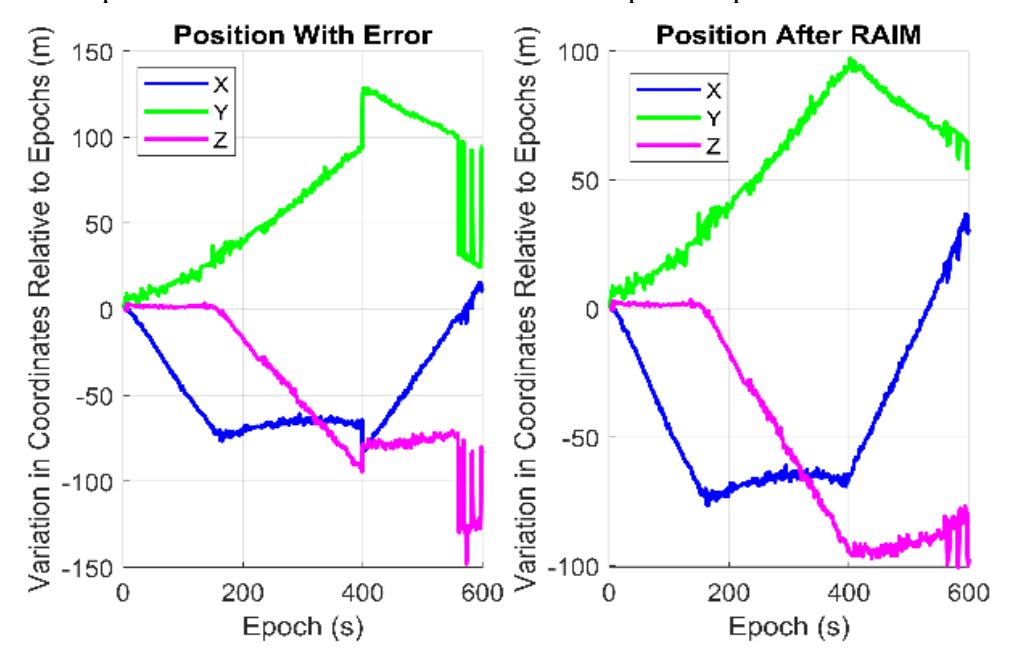


Figure 8: Comparison of variation in coordinates with respect to epochs

4.2. Data set-2

In order to confirm the working of the algorithm, another data set was collected at different time. During this data set the global test detected an error in epoch 150 and onwards and an alarm was generated. After the global test, this time the PRN 21 was found to be the satellite with erroneous measurements which was identified through the fault identification tests. Figures 9 and 10 shows the results obtained through global test and protection levels respectively. Furthermore, the results of the identification tests can be observed in the Figure 11. Similarly, in Table-3 it can be observed that the PRN 21 (satellite with erroneous measurements) has higher values obtained through the LSR testing and the correlation coefficient while a minimum value in case of the correlation distance.

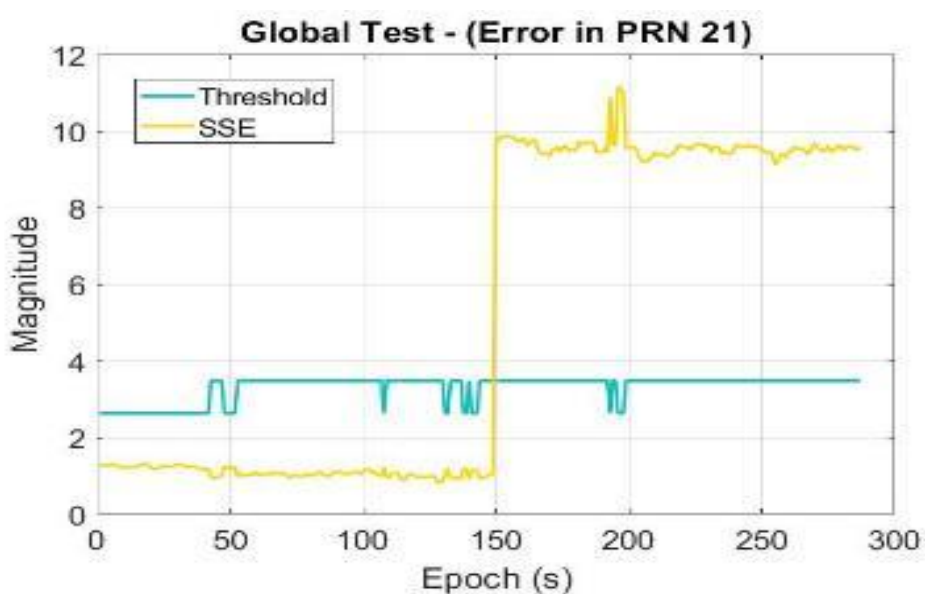
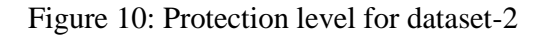


Figure 9: Global test for dataset-2



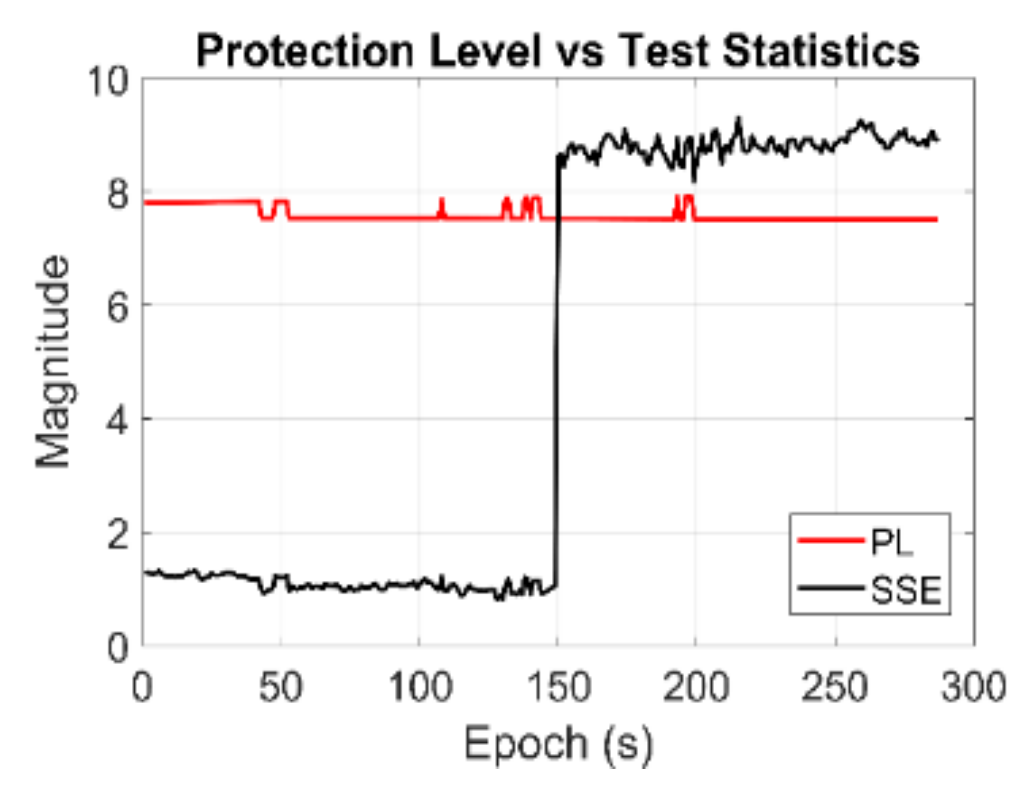
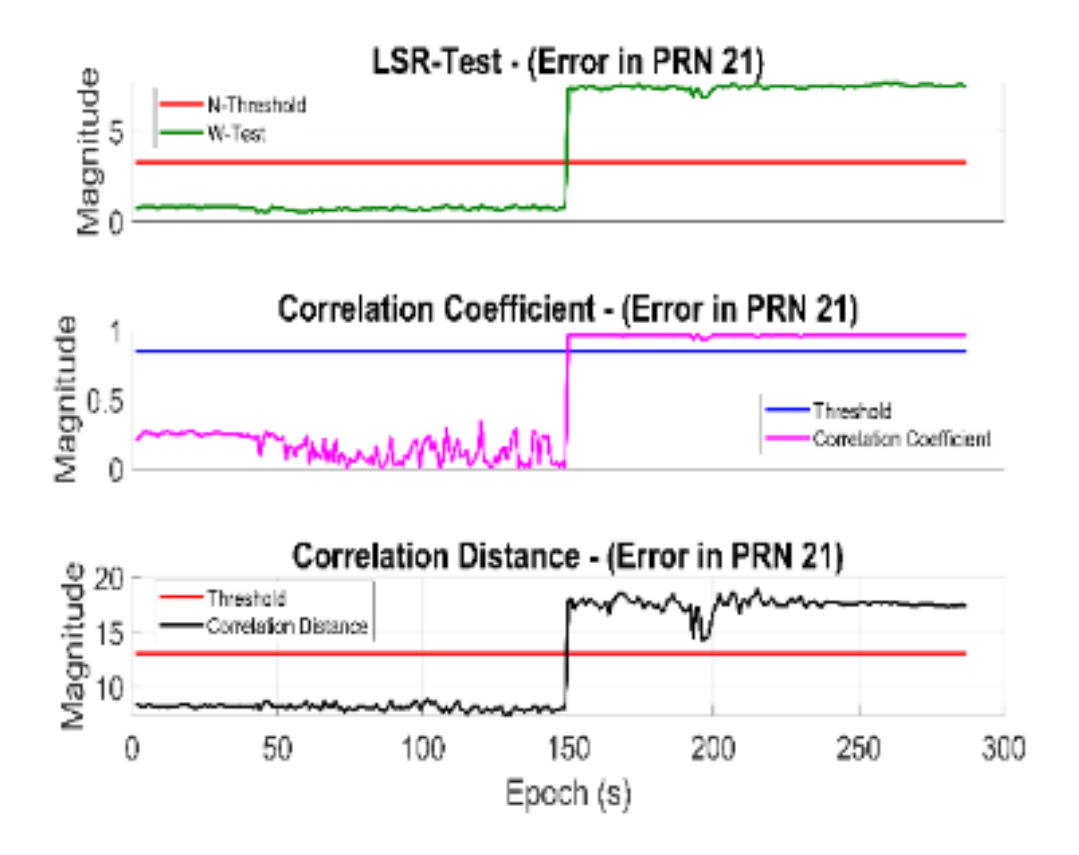


Figure 11: Fault identification for Dataset-2

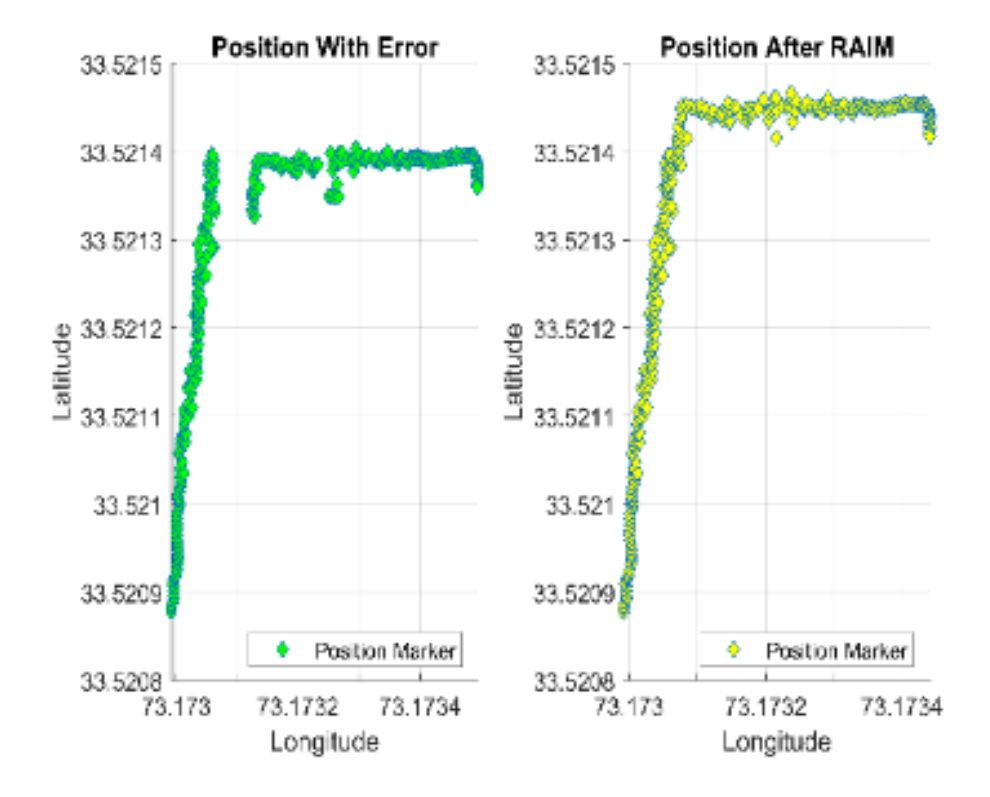


The position calculated with and without erroneous measurements can be observed in the Figure 12.

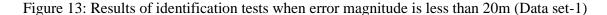
Table-3: Test resu	ılts for	fault	identi	fication	(Dataset-2)

Satellite (PRN)	LSR Testing	Correlation Coefficient	Correlation Distance
32	1.3997	0.1744	17.332
22	0.7573	0.0480	16.807
10	2.0418	0.2194	17.447
23	0.7402	0.0434	16.572
21	7.4697	0.9564	9.905
31	0.7258	0.2213	17.918
27	0.7287	0.0098	17.304
8	4.5948	0.1736	18.611
24	1.7540	0.0426	18.426
18	2.1970	0.3945	19.292
1	2.8541	0.6295	55.540

Figure 12: Comparison of position with and without error



Furthermore, in order to determine the response of the algorithm to errors of various magnitudes, the intentionally error was varied gradually and the results were observed carefully. It was found that the error with a magnitude greater than 20 meter, the success rate of detection and identification was 100%. However, as the magnitude of error dropped below 20 meters, the success rate of LSR test was decreased and it resulted in the false alarm and false detection as seen in the Figures 13 and 14 for both data sets respectively. Thus, it is better to rely on the results obtained from multiple tests for fault identification and exclusion rather than a single test only.



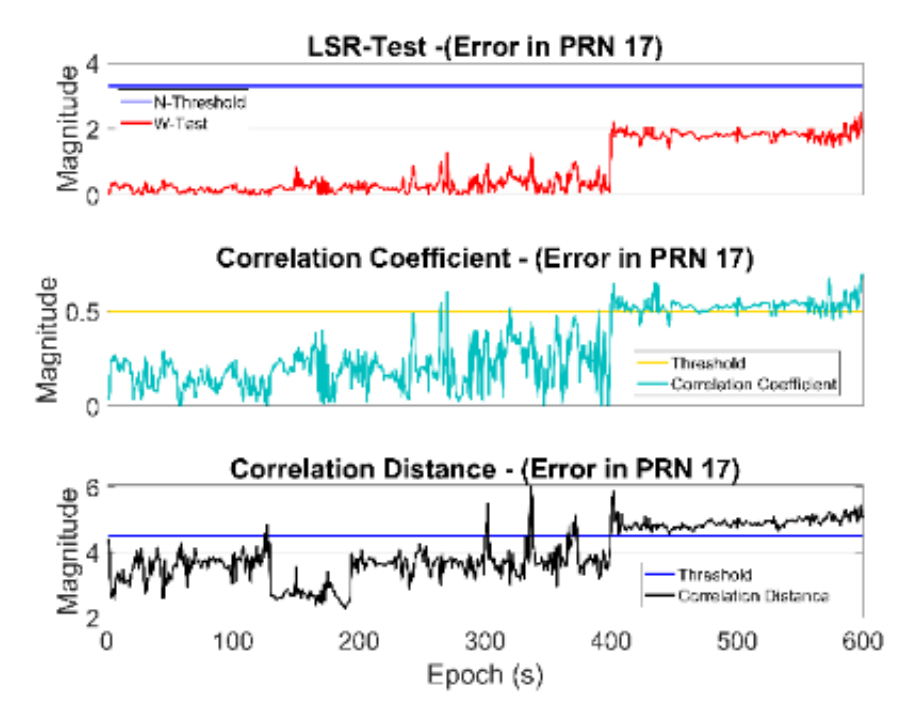
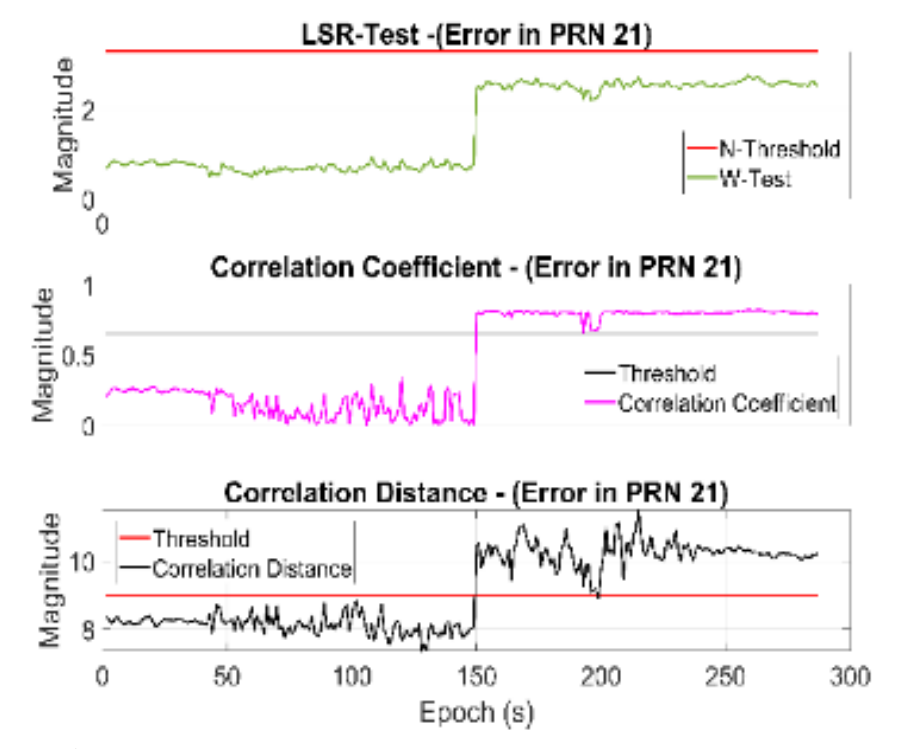


Figure 14: Results of identification tests when error magnitude is less than 20m (Data set-2)



5. Conclusion

From the results obtained during this experiment, it has been found that a single test for fault detection and exclusion may not be sufficient as it can sometime result in false alarms and false detection. An integrity algorithm based on multiple tests was introduced which improves the accuracy of fault detection and exclusion. Instead of relying on the decision from a single test,

a voting scheme has been introduced which involves the decision from three different tests among which at least 2 tests must be consecutively pointing to the same PRN. Furthermore, in case of random errors, the exclusion of satellites should be done in a controlled manner in order to avoid the inconsistency of the geometry required for position calculation. In addition to this, the proposed algorithm can also be backed with additional features such as Non-Line Of Sight (NLOS) classifier to further improvise the positioning accuracy in case of multipath scenario when the receiver is under dense urban canyon.

Acknowledgements

- a) The authors are thankful to National Centre of GIS and Space Applications (NCGSA) and GNSS Space Education Research Lab (GSERL) for providing GNSS receivers and equipment required for conducting this research.
- b) A partial data, results and analysis of this manuscript have been presented by the authors in the 19th International Bhurban Conference on Applied Sciences and Technology (IBCAST), 2022 with title: "GNSS Fault Detection and Exclusion Algorithm for Single Frequency Receivers".

Declaration of conflict of interest

The author(s) declared no potential conflicts of interest(s) with respect to the research, authorship, and/or publication of this article.

ORCID iD

Sunnayaha Saeed https://orcid.org/0000-0001-9977-5284

Evaluation of the weighted least square based Receiver Autonomous integrity Monitoring ...

References

- Angrisano, A., Gaglione, S., & Gioia, C. (2012). RAIM algorithms for aided GNSS in Urban scenario. In 2012 Ubiquitous Positioning, Indoor Navigation, and Location Based Service, (UPINLBS), 1-9. https://doi.org/10.1109/UPINLBS.2012.6409786
- Baarda, W. (1968). A testing procedure for use in geodetic networks. *Publications on Geodesy*, 2(5), 97.
- Blanch, J., Walter, T., Enge, P., & Kropp, V. (2015). A simple position estimator that improves advanced RAIM performance. *IEEE Transactions on Aerospace and Electronic Systems*, 51(3), 2485–2489. https://doi.org/10.1109/TAES.2015.140674
- BROWN, R. G. (1992). A baseline GPS RAIM scheme and a note on the equivalence of three RAIM Methods. *Navigation*, 39(3), 301–316. https://doi.org/10.1002/j.2161-4296.1992.tb02278.x
- Farooq, S. Z., Ada, E. N. J., & Yang, D. (2020). Design and implementation of single frequency RTK positioning framework. *Proceedings of the International Astronautical Congress, IAC*, 2020(October), 12–14.
- Farooq, S. Z., Yang, D., & Ada, E. N. J. (2020). A cycle slip detection framework for reliable single frequency RTK positioning. *Sensors (Switzerland)*, 20(1), 304. https://doi.org/10.3390/s20010304
- Hawkins, D. M. (1980). *Identification of outliers*. Springer. https://doi.org/10.1007/978-94-015-3994-4
- Hewitson, S., & Wang, J. (2006). GNSS receiver autonomous integrity monitoring (RAIM) performance analysis. *GPS Solutions*, 10(3), 155–170. https://doi.org/10.1007/s10291-005-0016-2
- Imtiaz, H., Haroon Yousaf, M., Sajjad Malik, H., & Ali Akhtar, M. (2019). Design and implementation of receiver autonomous integrity monitoring algorithm on DSP for small UAV applications. *Proceedings 2019 International Conference on Frontiers of Information Technology, FIT 2019*, 278–283. https://doi.org/10.1109/FIT47737.2019.00059
- Joerger, M., & Pervan, B. (2013). Kalman filter-based integrity monitoring against sensor faults. *Journal of Guidance, Control, and Dynamics*, *36*(2), 349–361. https://doi.org/10.2514/1.59480
- Kaplan, E. D., & Hegarty, C. J. (2017). *Understanding GPS/GNSS principles and applications* (3rd Edition). Artech House.
- Kuusniemi, H. (2005). User-level reliability and quality monitoring in satellite-based personal navigation. *Tampere University*.
- Lee, Y. (1986). Analysis of range and position comparison methods as a means to provide GPS integrity in the user receiver. *Navigation Journal of the Institute of Navigation*, 1–17. http://wwwsrv1tmp.mitre.org/work/best_papers/98/winner_lee/winner_lee.pdf
- Lee, Y. C. (1992). Receiver Autonomous Integrity Monitoring (RAIM) capability for solemeans GPS navigation in the oceanic phase of flight. *IEEE Aerospace and Electronic Systems Magazine*, 7(5), 29–36. https://doi.org/10.1109/62.257089
- Ma, X., Yu, K., Montillet, J. P., & He, X. (2019). Equivalence proof and performance analysis of weighted least squares residual method and weighted parity vector method in RAIM. *IEEE Access*, 7, 97803–97814. https://doi.org/10.1109/ACCESS.2019.2929073
- Parkinson, B. W., & Axelrad, P. (1988). Autonomous GPS integrity monitoring using the pseudorange residual. *Navigation*, *35*(2), 255–274. https://doi.org/10.1002/j.2161-4296.1988.tb00955.x

- Rakipi, A., Kamo, B., Cakaj, S., Kolici, V., Lala, A., & Shinko, I. (2015). Integrity monitoring in navigation systems: Fault detection and exclusion RAIM algorithm implementation. *Journal of Computer and Communications*, 3(06), 25–33. https://doi.org/10.4236/jcc.2015.36004
- Santa, J., Úbeda, B., Toledo, R., & Skarmeta, A. F. G. (2006). Monitoring the position integrity in road transport localization based services. *IEEE Vehicular Technology Conference*, *October*, 2801–2805. https://doi.org/10.1109/VTCF.2006.575
- Sturza, M. A. (1988). Navigation system integrity monitoring using redundant measurements. *Navigation*, *35*(4), 483–501. https://doi.org/10.1002/j.2161-4296.1988.tb00975.x
- Sun, Q., & Zhang, J. (2009). RAIM method for improvement on GNSS reliability and integrity. In *AIAA/IEEE Digital Avionics Systems Conference-Proceedings*, 1–11. https://doi.org/10.1109/DASC.2009.5347420
- Teunissen, P. J. G., & Montenbruck, O. (Eds.). (2017). *Springer handbook of global navigation satellite systems*. Springer. https://doi.org/10.1007/978-3-319-42928-1
- Teunissen, P. J. G. (1990). Quality control in integrated navigation systems. *IEEE Aerospace and Electronic Systems Magazine*, 5(7), 35–41.
- Wang, E., Yang, F., & Pang, T. (2018). GNSS receiver autonomous integrity monitoring algorithm based on least squared method. In *Proceedings of the 2017 12th IEEE Conference on Industrial Electronics and Applications, ICIEA 2017*, 2018-Febru(1), 2017–2021. https://doi.org/10.1109/ICIEA.2017.8283169
- Zabalegui, P., De Miguel, G., Perez, A., Mendizabal, J., Goya, J., & Adin, I. (2020). A review of the evolution of the integrity methods applied in GNSS. *IEEE Access*, 8, 45813–45824. https://doi.org/10.1109/ACCESS.2020.2977455
- Zhang, Q., Zhao, L., & Zhou, J. (2019). Improved method for single and multiple gnss faults exclusion based on consensus voting. *Journal of Navigation*, 72(4), 987–1006. https://doi.org/10.1017/S0373463318001133
- Zheng, X., Liu, Y., Fan, G., Zhao, J., & Xu, C. (2018). Analyses of the sensitivity of multi-constellation advanced receiver autonomous integrity monitoring vertical protection level availability to error parameters and a failure model over China. *Advances in Mechanical Engineering*, 10(6), 1–11. https://doi.org/10.1177/1687814018776191
- Zhu, N., Betaille, D., Marais, J., & Berbineau, M. (2018). GNSS integrity enhancement for urban transport applications by error characterization and Fault Detection and Exclusion (FDE). *URSI-France 2018 Workshop: Geolocation and Navigation in Space and Time*, 1–11.
- Zhu, N., Betaille, D., Marais, J., & Berbineau, M. (2020). GNSS integrity monitoring schemes for terrestrial applications in harsh signal environments. *IEEE Intelligent Transportation Systems Magazine*, 12(3), 81–91. https://doi.org/10.1109/MITS.2020.2994076

Appendix: List of abbreviations

GNSS: Global Navigation Satellite Systems

GPS: Global Positioning System

RAIM: Receiver Autonomous Integrity Monitoring SBAS: Satellite Based Augmentation System GBAS: Ground Based Augmentation System

PL: Protection Level

VPL: Vertical Protection Level HPL: Horizontal Protection Level LSR: Least Square Residual PRN: Pseudorandom Noise

RINEX: Receiver Independent Exchange Format

SSE: Sum of Squared Residual **P**_{FA}: Probability of False Alarm PMD: Probability of Missed Detection

ICAO: International Civil Aviation Organization

SV: Satellite Vehicle